Axonal growth of embryonic stem cell-derived motoneurons *in vitro* and in motoneuron-injured adult rats

James M. Harper*, Chitra Krishnan*, Jessica S. Darman†, Deepa M. Deshpande*, Schonze Peck*, Irina Shats*, Stephanie Backovic*, Jeffrey D. Rothstein*‡, and Douglas A. Kerr*†§

*Department of Neurology, Johns Hopkins University School of Medicine, Pathology 627C, 600 North Wolfe Street, Baltimore, MD 21287; †Department of Molecular Microbiology and Immunology, Johns Hopkins University Bloomberg School of Public Health, 615 North Wolfe Street, Baltimore, MD 21205; and ‡Department of Neurosciences, Johns Hopkins University School of Medicine, Meyer 6-109C, 600 North Wolfe Street, Baltimore, MD 21287

Edited by Solomon H. Snyder, Johns Hopkins University School of Medicine, Baltimore, MD, and approved March 22, 2004 (received for review February 16, 2004)

We generated spinal motoneurons from embryonic stem (ES) cells to determine the developmental potential of these cells *in vitro* and their capacity to replace motoneurons in the adult mammalian spinal cord. ES cell-derived motoneurons extended long axons, formed neuromuscular junctions, and induced muscle contraction when cocultured with myoblasts. We transplanted motoneuron-committed ES cells into the spinal cords of adult rats with motoneuron injury and found that ≈3,000 ES cell-derived motoneurons (25% of input) survived for >1 month in the spinal cord of each animal. ES cell-derived axonal growth was inhibited by myelin, and this inhibition was overcome by administration of dibutyryl cAMP (dbcAMP) or a Rho kinase inhibitor *in vitro* and *in vivo*. In transplanted rats infused with dbcAMP, ≈80 ES cell-derived motor axons were observed within the ventral roots of each animal, whereas none were observed in transplanted rats not treated with dbcAMP. Because these cells replicate many of the developmental and mature features of true motoneurons, they are an important biological tool to understand formation of motor units *in vitro* and a potential therapeutic tool to reconstitute neural circuits *in vivo*.

Embryonic stem (ES) cells are pluripotent cells that are both self-renewing and have the capacity to differentiate into any cell type in the adult organism. They can be propagated *in vitro* for long periods of time in an undifferentiated state and thus represent an attractive source of cells for developmental studies and for therapy of human diseases. ES cells are responsive to environmental cues upon transplantation and adopt a cellular fate that is appropriate to the transplanted region (1–6). Nevertheless, the dependence on environmental cues to direct stem cells precludes the efficient generation of neurons in nonneurogenic regions of the CNS (3, 7).

Recently, it has become possible to direct the differentiation of stem cells *ex vivo*, theoretically making these cells less dependent or independent of *in vivo* cues. Differentiating ES cells express developmentally appropriate transcription patterns (8) and are capable of carrying out functions of mature neural cells upon transplantation (9, 10). Other signals given *in vitro* can also induce specific neural fates upon transplantation. For example, fibroblast growth factor, heparin, and laminin can be used to induce neurally committed stem cells to adopt cholinergic neural fates upon transplantation (11).

Spinal motoneurons can be generated efficiently by exposing mouse ES cells to retinoic acid (RA) and Sonic hedgehog (12). In this paradigm, RA serves both to neuralize and to establish a caudal positional identity for the pluripotent ES cells. Sonic hedgehog or Hedgehog agonist (HhAg1.3) further specifies a ventral positional identity and in response, a substantial proportion of ES cells initiate a motor neuron-specific transcriptional pattern and acquire immunohistochemical features of mature neurons. ES cell-derived motoneurons transplanted into embryonic chick spinal cord extend axons into the periphery and form neuromuscular junctions.

The implications of this finding are two-fold. First, the study of developing ES cell-derived motoneurons may result in important insight into molecular mechanisms that underlie motoneuron function. With this system, it may be possible to investigate critical pathways involved in the establishment and maintenance of motoneurons, and to determine where these pathways are disrupted in genetic models of motoneuron disease. Second, ES cell-derived motoneurons may be examined for their therapeutic potential to reconstitute motor units in motoneuron diseases. To be considered as a viable therapeutic strategy, however, ES cell-derived motoneurons must not only survive within the spinal cord but also be able to extend axons through surrounding white matter into peripheral nerves and reinnervate anatomically appropriate targets. None of these steps has currently been shown in the adult mammalian nervous system.

We investigated the potential use of ES cell-derived motoneurons as a biological tool to study motor neuron development and as a therapeutic strategy in paralyzed animals. We found that ES cell-derived motoneurons extended long axons, established neuromuscular junctions, and induced muscle contractions with cocultured myoblasts *in vitro*. Transplantation of motoneuron-committed ES cells into adult rat spinal cord resulted in the generation and long-term survival of ES cell-derived motoneurons. Furthermore, ES cell-derived axonal growth was inhibited by myelin and this inhibition can be partially overcome by pharmacologic treatment of host animals. We conclude that ES cell-derived motoneurons exhibit features of native motoneurons and represent an attractive model system for examining motoneuron development and potential therapeutic strategies for motor neuron diseases.

Methods

Reagents. Antibodies and dilutions used in this study include the following: AB1982 neurofilament 200KD (Chemicon, 1:500); SMI 31/neurofilament (Sternberger Monoclonals; 1:2,000); MAB368 synaptophysin (Chemicon, 1:1,000); AGR-510 agrin (all agrin; Stressgen, 1:500); AGR-520 neural agrin (Stressgen, 1:500); MMS-627R acetylcholine R7 α-subunit (Covance Research, 1:1,000); M6 (mouse-specific immunoreactivity; Developmental Studies Hybridoma Bank 1:1,000); and rhodamine-conjugated bungarotoxin was purchased from Molecular Probes (T-1175; 1:1,000). HhAg1.3 (Curis) was made up as a 10-mM stock in DMSO and was used at 1 μM. All-trans RA (Sigma R-2625) was made up as a 1-mM stock in DMSO and used at 1 μM. Dibutyryl cAMP (dbcAMP) was

This paper was submitted directly (Track II) to the PNAS office.

Abbreviations: ES, embryonic stem; dbcAMP, dibutyryl cAMP; PLL, poly-L-lysine; NSV, neuroadapted Sindbis virus.

§To whom correspondence should be addressed. E-mail: dkerr@jhmi.edu.

© 2004 by The National Academy of Sciences of the USA

obtained from Calbiochem (catalog no. 28745). Y27632 (Calbiochem) was made up at 2 μg/μl in sterile distilled water (13).

Microscopy. Immunohistochemical studies were carried out by two-color confocal imaging with a Zeiss LSM510 microscope. Images were acquired in both red and green emission channels by using an argon-krypton laser with a single-channel, line-switching mode.

***In Vitro* Myelin Inhibition.** Myelin was extracted from adult rat brain as described (14). Neurite outgrowth was quantified by using IMAGE J, a public domain JAVA image processing program (http://rsb.info.nih.gov/ij). Neurons and their axons were identified by using the fluorescence produced by GFP expressed from the HB9 promoter. Axon length was determined by tracing and recording the length of all GFP$^+$ axons. Cells that did not produce axons were given a set value near zero. Cells with axons that were not in full view were not included. Total neurite length was then divided by the total number of cells, generating a mean axon length per cell within each test group. The SEM was determined and mean neurite outgrowth was plotted as a percentage of the control group. Two evaluators (S.P. and J.M.H.) determined the neurite length blinded to the treatment groups and obtained similar results.

Cell Culture. ES cell motoneuron differentiation was carried out as previously reported with slight modifications (12). ES cells were exposed to RA/Sonic hedgehog for 3 days, after which they were disaggregated with collagenase and dispase and plated on confluent astrocytes. For Campenot chambers, we used a modified Camp3 (Tyler Research) in which the central septa were almost completely removed. We then placed a no. 2 glass coverslips with silicone grease onto the original septae overhang and lowered it to the dish surface. Silicone grease was placed on the bottom surface of the coverslip to eliminate leakage between chambers. The myoblast chambers were coated with poly-L-lysine (PLL)/laminin and the astrocyte chambers and middle chambers were coated with collagen. C2C12 myoblasts were purchased from American Type Culture Collection. The day after astrocyte plating, myoblasts and ES cells were plated in distinct chambers. The following day, myoblast differentiation medium (DMEM plus 2% normal horse serum) was added to the appropriate chamber and myoblast differentiation was allowed to continue for 3–5 days. When multinucleated skeletal myotubes first began to form, the glass septa dividing the chambers was raised, bringing the chambers into continuity.

Transplantation. Five- to 7-week-old male Lewis rats were used for transplantation studies. Rat-adapted neuroadapted Sindbis virus (NSV) was generated and used as described (6). Briefly, rats were given 5,000 plaque-forming units of NSV by means of intracranial inoculation; paralysis occurred within 7 days of viral inoculation. Transplantation was carried out at 14–17 days after viral inoculation ($n = 10$). Rats were anesthetized with 1% isoflurane and a two-level laminotomy exposed the lumbar enlargement. After incision of the dura, 60,000 motoneuron-committed ES cells in 2 μl were injected into the ventral gray matter (0.7 mm lateral to the midline, and a depth of 1.5 mm from the dorsal surface of the spinal cord). All rats were given cyclosporine (Calbiochem) at 10 mg per kg per day on the day before surgery/transplantation, then every day after surgery.

Immunohistochemistry. Animals were perfused at 1 month after transplantation with 4% paraformaldehyde. By use of the sciatic nerve to identify L3-L5, the rostral border of the spinal cord was sectioned beginning at L1 (two ventral roots more rostral than the sciatic nerve contributions). All ventral roots from the lumbar and caudal spinal cord were harvested and were examined by immunohistochemistry for colocalized GFP and neurofilament staining to identify ES cell-derived axons. For estimation of surviving ES cell-derived motoneurons within transplanted spinal cords, every 10th 20-μm section was placed on a glass slide and examined for GFP immunoreactivity. GFP$^+$ cell bodies were counted and the mean per animal was calculated (three animals per group). To estimate the total number of surviving transplanted cells, we multiplied the calculated number by 10.

***In Vivo* Axonal Growth.** For stimulating axonal outgrowth, we purchased 5- to 7-week-old Lewis rats that had been cannulated into the lumbar intrathecal space (Zivic–Miller). A subset of these animals was given NSV to induce paralysis before transplantation. All cannulated rats were transplanted simultaneously with ES cells and a 1007D Alzet pump (0.5 μl/h for 7 days) was attached to the CSF cannula. Animals received PBS (six animals), Y-27632 (six animals, 170 μg per rat over 1 week), or dbcAMP (six animals, 175 μg per rat over 1 week).

Results

ES cells in this study were derived from an HB9-GFP-transgenic mouse and fluoresced green upon adoption of a motoneuron phenotype (12). To enhance the differentiation and survival of ES cell-derived motoneurons, we modified a previously published protocol (12) by trypsinizing ES cells 3 days after exposing them to HhAg1.3 and RA and plating them on a confluent bed of astrocytes (see Fig. 6, which is published as supporting information on the PNAS web site). Approximately 25–30% of cells coexpressed high levels of HB9, or Islet 2 and GFP under control of the HB9 promoter. The HB9-GFP$^+$ cells also strongly expressed neuronal nuclear protein, neurofilament, and choline acetyltransferase (Fig. 6).

To further determine the potential of motoneuron-committed ES cells, we developed a coculture system that included skeletal muscle-differentiated C2C12 myoblasts. C2C12 myoblasts exposed to 2% normal horse serum fused and formed elongated myotubes (Fig. 1*A*) and expressed skeletal muscle-specific troponin T and myosin heavy chain (Fig. 1*B*). We used a modified Campenot chamber (15) in which a glass coverslip initially separated two chambers, one with differentiating myoblasts and the other with disaggregated, HhAg1.3/RA-treated ES cells plated on an astrocyte monolayer. One day after plating the ES cells, the glass coverslip separating the two chambers was gently raised, allowing the two chambers to come into continuity with each other. Within 2–3 h, the motoneuron-differentiated ES cells began to extend processes toward the adjacent chamber, and within $\approx$24–30 h began reaching the adjacent chamber.

We explored whether this coculture system induced cellular changes that recapitulate those involved in the formation of neuromuscular junctions, which is a complex, mutually inductive process that involves numerous signaling pathways initiated by both the muscle and the neuron. At various times after bringing the chambers into continuity, we again separated them to generate muscle-enriched or motoneuron-enriched lysates (Fig. 1*C*). Agrin, a proteoglycan produced by motoneurons and by muscle, is secreted during development and is required for postsynaptic differentiation (16, 17). Expression of agrin in the muscle chamber was markedly up-regulated within 2 h of coculture and remained elevated through the period when ES cell-derived axons began making contact with muscle. We also saw a progressive up-regulation of the acetylcholine receptor α7 subunit and skeletal actin within the muscle lysate, suggesting that the presence of cocultured motoneurons induced further differentiation and organization of skeletal myotubes (Fig. 1*C*). Neural agrin is an alternatively spliced isoform that is generated within neurons and markedly enhances organization of the postsynaptic membrane and induction of synaptic vesicle clustering within the motoneuron itself (18). Neural agrin was expressed at low levels in independently differentiating ES or C2C12 myoblasts (Fig. 1*C*, ES or MU, left two lanes). Within the neural chamber, however, neural agrin was markedly up-regulated within 2 h of

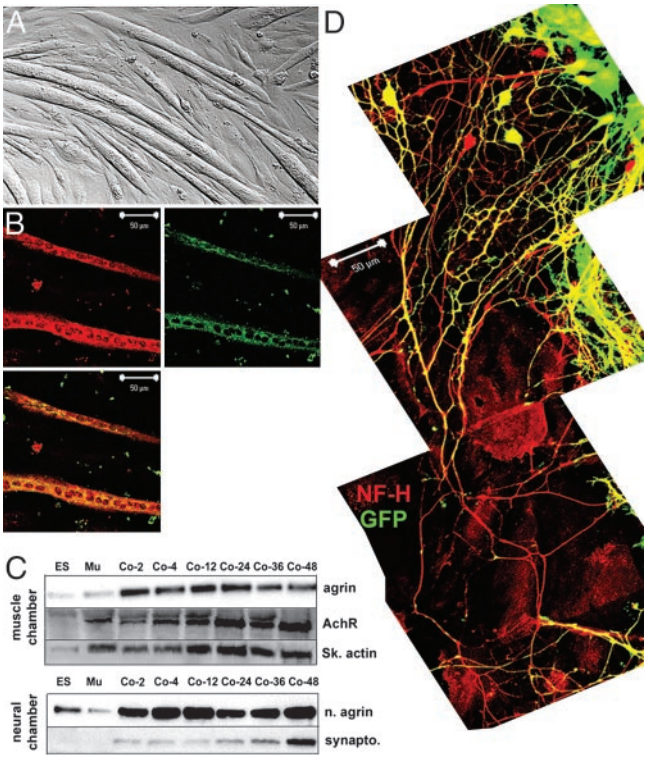

Fig. 1. Coculture of ES cell-derived motoneurons and differentiated C2C12 myoblasts. C2C12 myoblasts were plated in a modified Campenot chamber and were exposed to differentiation conditions. (*A*) Three to five days after switching to differentiation medium, C2C12 myoblasts became elongated, which is consistent with multinucleated myotubes. (*B*) Differentiated myotubes expressed skeletal muscle-specific proteins, including skeletal myosin heavy chain and troponin T, and are multinucleated. (*C*) In an adjacent chamber of the Campenot dish, ES cells were differentiated into motoneurons as described. At 3 days after exposure of ES cells to HhAg1.3/RA, the glass septa dividing the chambers was raised, bringing the chambers into continuity. Cell lysates were generated from ES/astrocyte cultures or from myoblast cultures at various times after bringing the chambers into continuity. ES, lysates from the ES chamber; MU, lysates from the muscle chamber at time 0 (before initiating coculture). Agrin, acetylcholine receptor, and skeletal muscle actin were up-regulated rapidly within the muscle chamber; neural agrin and synaptophysin were up-regulated within the ES/astrocyte chamber. (*D*) Upon coculture, motoneuron-committed ES cells extended long axons (900 μm in length here) toward the myoblast chamber (*Lower*) that were both GFP$^+$ and neurofilament-H$^+$ (red). Axonal processes reached lengths of 3–5 mm (data not shown).

coculture. Synaptophysin, a presynaptic vesicle protein, was up-regulated only at the end of the examined coculture period, suggesting that after making initial contact with the muscle, the motoneurons were further developing the machinery to carry out synaptic activity. The simplest explanation for these findings is that the motoneuron-differentiated ES cells and the skeletal myotubes respond to each other by beginning to form neuromuscular junctions.

Morphologically, motoneuron-differentiated ES cells extended long axons up to 3–5 mm into the adjacent chamber (Fig. 1*D* and data not shown). In the confocal photomicrograph collage (Fig. 1*D*), the muscle chamber was below the bottom image. The astrocyte:motoneuron chamber is shown at the top with some single and a few clusters of GFP$^+$ cells. Processes extended directionally toward the muscle chamber and expressed both GFP and neurofilament 200 (here shown extending 900 μm). Therefore, morphologic and biochemical evidence suggests that ES cell-derived motoneurons undergo biochemical and morphologic changes in response to cocultured muscle, resulting in axon growth directed toward skeletal myotubes.

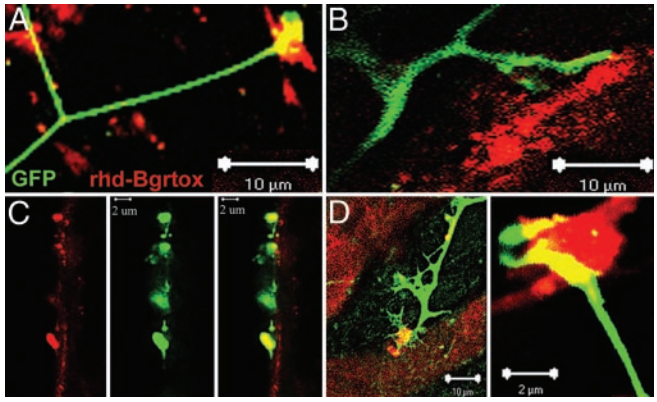

Fig. 2. ES cell-derived motoneurons form neuromuscular junctions with cocultured myoblasts. Two days after coculture, myoblasts could be seen irregularly contracting throughout the dish (see Movie 2, which is published as supporting information on the PNAS web site). (*A–E*) Confocal microscopy reveals colocalization or close apposition of GFP$^+$ axons with rhd-conjugated bungarotoxin. In *C*, a 0.4-μm confocal section derived from a Z stack shows clustering of acetylcholine receptors as the GFP axons make contact with the surface of myotube (vertically oriented).

To examine whether ES cell-derived axons could form neuromuscular junctions with cocultured muscle, we attempted to colocalize GFP$^+$ axons with rhd-bungarotoxin. Because bungarotoxin derivatives identify clustered acetylcholine receptors (19, 20), such colocalization would imply that the cocultured cells can organize a neuromuscular junction appropriately. Indeed, by 48 h after coculture, we saw extensive colocalization of GFP$^+$ axons with rhd-bungarotoxin (Fig. 2). Some GFP$^+$ axons (Fig. 2 *A*, *D*, and *E*) exhibited terminal enlargements as they made contacts with the surface of cocultured myotubes. Single 0.3-μm images of a confocal Z stack image (Fig. 2*C*) revealed that axon terminals (here descending into the plane of the photomicrograph) may colocalize with multiple acetylcholine receptor clusters on a single myotube.

Consistent with the observation that cocultured ES cell-derived motoneurons and skeletal myotubes can form neuromuscular junctions, 30% of skeletal myotubes routinely and asynchronously contracted in the tissue culture dish, beginning 48 h after establishment of coculture (Movie 1, which is published as supporting information on the PNAS web site). C2C12 myoblasts did not contract in the absence of cocultured motoneurons nor did they contract in response to conditioned media from ES cell-derived motoneurons. Further, muscle contraction was completely inhibited by incubating with tubocurarine, a competitive inhibitor of nicotinic acetylcholine receptors (data not shown), suggesting that acetylcholine release from ES cell-derived motoneurons was responsible for the muscle contraction.

We next determined whether motoneuron-committed ES cells survived and differentiated appropriately within the spinal cord of a paralyzed adult rat. We administered NSV intracranially to induce fulminant motor neuron death and permanent paralysis as described (6, 21). At 14–17 days after virus inoculation, animals showed nearly complete paralysis of hindlimbs while the virus was largely cleared. We transplanted 60,000 RA/HhAg1.3-treated ES cells directly into the lumbar ventral gray matter of adult Lewis rats 14–17 days after virus inoculation. Animals were killed 1 month later and were examined for the presence of GFP-expressing cells. We found GFP$^+$ cells within the lumbar enlargement, but there were no GFP$^+$ cells >5 mm rostral or caudal to the injection site, indicating little migration of the transplanted cells (Fig. 3*A*). Control transplantations, in which freeze-thaw-killed ES cells were implanted, showed no GFP fluorescence. Further, immunofluorescence with a mouse-specific antibody (M6), confirmed that these GFP$^+$ cells were of mouse origin and did not represent fusion with

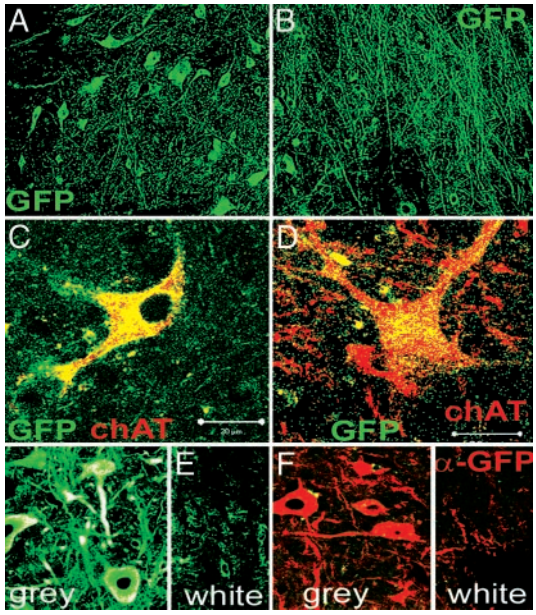

Fig. 3. Motoneuron-committed ES cells survive and express motoneuron markers in the adult mammalian spinal cord. A total of 60,000 ES cells were transplanted into the gray matter of the lumbar enlargement in NSV-paralyzed rats 3 days after exposure to HhAg1.3/RA. Animals were killed, and spinal cords were examined 1 month later. (*A*) GFP^+ cell bodies are seen throughout a portion of the gray matter of the lumbar enlargement extending ≈1–5 mm rostral and caudal to the injection site. (*B*) GFP^+ axonal processes extend throughout the gray matter of the same area. (*C* and *D*) Some GFP^+ cell bodies are large (>30 μm), morphologically resemble motoneurons and express choline acetyltransferase. (*E* and *F*) Sagittal sections of spinal cords show that most GFP^+ axons extend within the gray matter and relatively few extend into the surrounding white matter.

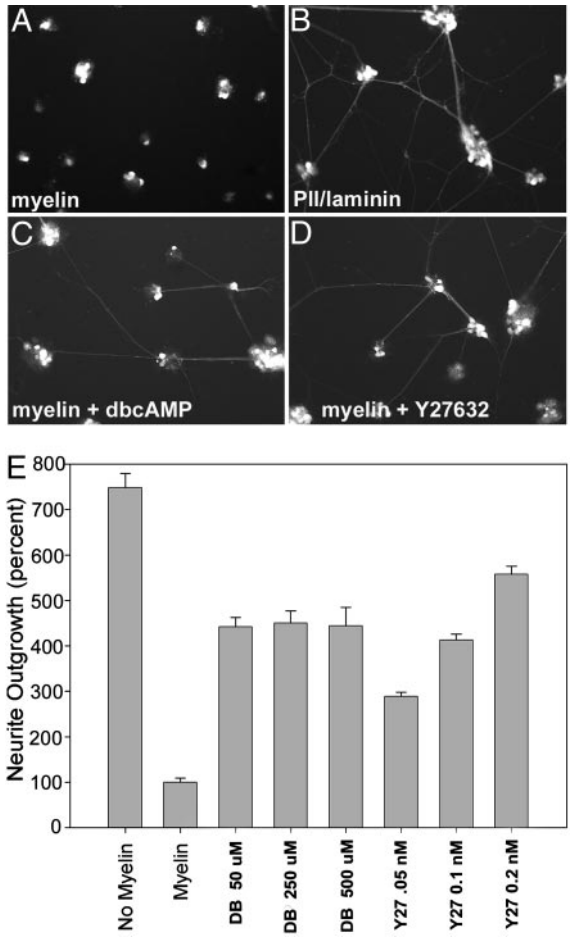

Fig. 4. Myelin-mediated axonal inhibition of ES cell-derived motoneurons *in vitro*. ES cells were plated on PLL/laminin-coated dishes that were then coated with myelin (*A*) or on PLL/laminin-coated dishes (*B*) 3 days after exposure to HhAg1.3/RA. Extensive axonal growth is seen only on PLL and laminin, suggesting that myelin inhibits axonal growth of ES cell-derived motoneurons. (*C–E*) Partial restoration of axonal growth when ES cell-derived motoneurons were plated on myelin in the presence of dbcAMP or Y-27632.

rat cells (data not shown). Within the transplanted region, extensive GFP axonal projections were seen throughout the gray matter, some of which extended up to 1 cm rostral or caudal to the transplantation site (Fig. 3*B* and data not shown). Because the primary method for detecting transplanted cells was expression of GFP, we do not know the total number of transplanted cells that survived within the spinal cords of transplanted animals. By carrying out an unbiased sampling of every 10th section within the lumbar spinal cord, however, we estimated that there was a mean survival of ≈3,096 ± 56 GFP^+ cells per spinal cord. Because transplanted cells are exiting the cell cycle (12), this number is likely to reflect largely survival of input cells rather than cells that replicated after transplantation. Furthermore, because ≈20% of ES cells express GFP under our differentiation conditions, we predicted that ≈12,000 transplanted cells would have expressed GFP had they all survived, and therefore, that ≈25% of transplanted cells survived to 1 month after transplantation. A similar analysis in nonparalyzed animals resulted in enhanced survival of transplanted cells (mean 4,956.7 ± 10 cells per spinal cord), suggesting that the microenvironment within the transplanted field was less supportive of transplanted cell survival in virus-paralyzed animals.

Many of the surviving GFP^+ cells expressed choline acetyltransferase and morphologically resembled true motoneurons (Fig. 3 *C* and *D*). Interestingly, in both normal and paralyzed animals, very few of the transplanted cells extended axons into the surrounding white matter (Fig. 3 *E* and *F*). Rather, most axonal projections were directed in the rostral-caudal projection (Fig. 3 *B*, *E*, and *F*) or deeper into the gray matter (Fig. 3 *E* and *F*).

This result raised the possibility that similar to other CNS neurons, ES cell-derived motoneurons were inhibited by myelin. We investigated this possibility by plating motoneuron-committed ES cells on a myelin substrate (22). We found that although cells adhered to this substrate, they extended axonal projections only inefficiently (compare Fig. 4 *A* with *B*). Myelin-mediated axonal repulsion of other neuronal populations is reduced by increased intracellular cAMP levels or by decreased Rho kinase activity. Therefore, we investigated whether ES cell-derived motoneurons responded in the same way. Indeed, treatment of ES cell-derived motoneurons with a nonhydrolyzable cAMP analogue (dbcAMP) or a Rho kinase inhibitor (Y27632) *in vitro* resulted in enhanced axonal extension on a myelin substrate (Fig. 4 *C* and *D*). Quantification of axonal extension revealed a non-dose-dependent 4-fold increase in axonal extension in the presence of dbcAMP (Fig. 4*E*). Similarly, Y27632 resulted in a 3- to 5-fold increase in axonal extension. Therefore, ES cell-derived motoneurons respond to myelin-mediated axonal repulsion by processes similar to that reported with other neuronal populations.

We then used this information to examine whether we could modulate the apparent white matter repulsion of ES cell-derived axonal growth *in vivo*. Separately, we infused rats intrathecally with Y27632, dbcAMP, or vehicle for 7 days, beginning at the time of transplantation. As expected, surviving motoneuron-differentiated ES cells extended axons that were limited to the gray matter in vehicle-treated animals (Fig. 5*A*). In animals treated with the Rho

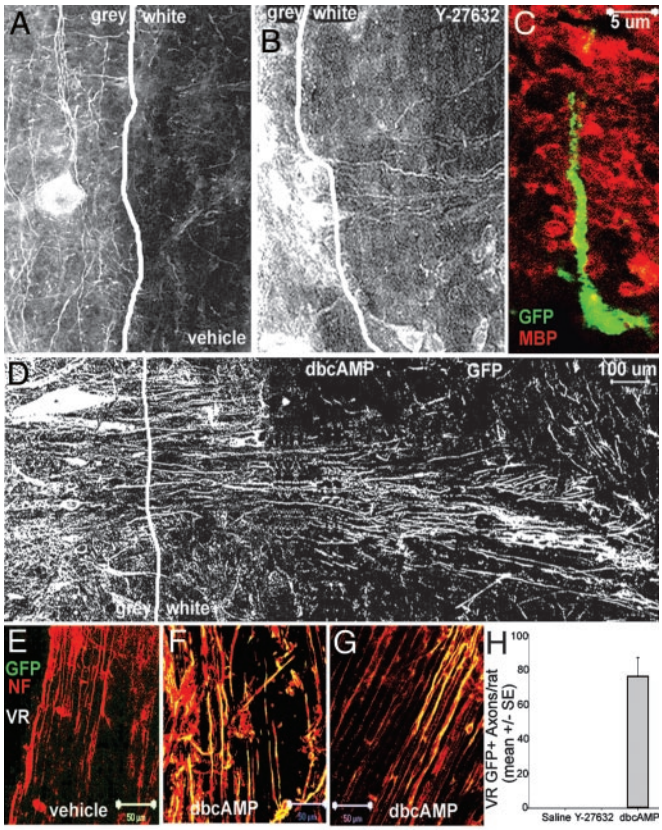

Fig. 5. ES cell-derived motoneurons extend axons into white matter and ventral roots in the presence of dbcAMP or Y27632. Transplantation of motoneuron-committed ES cells was repeated in spinal-cannulated, NSV-paralyzed rats. (*A*) In vehicle-infused rats, GFP$^+$ axons extend rostrally and caudally but only rarely extend into the surrounding white matter (sagittal section). (*B*) In Y27632-infused rats, GFP$^+$ axons traverse surrounding white matter. (*C*) Dual-color confocal microscopy confirms that GFP$^+$ axons extend into surrounding white matter, defined by immunoreactivity to myelin basic protein (red). (*D*) In dbcAMP-infused rats, axonal processes extend 1.3 mm to the surface of the spinal cord. (*E–H*) Ventral roots from the lumbar spinal cord were examined for the presence of GFP$^+$ axons at 1 month after transplantation. No GFP$^+$ axons are detected in vehicle-infused rats (*E*), whereas GFP$^+$ axons are detected within ventral roots of dbcAMP-infused rats (*F* and *G*). (*H*) Quantification of GFP$^+$ axons within ventral roots of transplanted animals. No GFP$^+$ axons within ventral roots were observed in paralyzed rats infused with either saline or with Y-27632, but a mean of 76 ± 10.69 GFP$^+$ axons were observed per transplanted rat infused with dbcAMP.

kinase inhibitor Y27632, however, a minority of GFP$^+$ axons could be seen traversing the white matter (Fig. 5*B*). No GFP$^+$ axons were identified within ventral roots of transplanted animals (data not shown). To confirm that we had correctly identified the gray-white junction, we carried out dual color immunohistochemistry against myelin basic protein and GFP (Fig. 5*C*). Most (but not all, see Fig. 5*B*) GFP$^+$ cell bodies were in the gray matter and some extended processes into an area rich in myelin basic protein (white matter). The effects of dbcAMP infusion *in vivo* were more pronounced than those seen with Y27632 and the majority of axons traversed the white matter (Fig. 5 *D* and *E*). GFP$^+$ cell bodies were observed near the gray-white junction and multiple GFP$^+$ processes extended into the white matter and even to the spinal cord surface (Fig. 5 *D* and *E*).

To estimate the frequency with which transplanted cells extended axons into the peripheral nervous system, we collected all of the ventral roots and examined them for GFP immunofluorescence. In uninfected (nonparalyzed) animals, no GFP$^+$ axons were seen in any ventral roots, even if the animal was concurrently treated with dbcAMP, suggesting that removal of myelin-mediated repulsion was insufficient to direct axonal growth. In paralyzed animals, no GFP$^+$ axons were seen within ventral roots in animals concurrently infused with saline (Fig. 5 *F* and *I*), whereas a mean of 76 ± 10.69 GFP$^+$ axons per animal were seen in paralyzed animals concurrently infused with dbcAMP (2.4% of surviving ES cell-derived motoneurons; Fig. 5 *G–I*). Therefore, removal of the inhibitory effects of myelin allowed for ES cell-derived axonal extension into ventral roots, albeit inefficiently. GFP$^+$ axons were confined to the proximal ventral roots, and no GFP$^+$ axons were observed >5 mm distal to the entry of that root into the spinal cord. Interestingly, no transplanted motor axons were seen in the ventral roots of Y-27632-infused animals, even though this was a more effective modifier of myelin repulsion *in vitro*. Currently, we do not understand the reasons for this discrepancy. Additionally, we did not see reinnervation of proximal muscles (data not shown).

Discussion

We investigated the biology of ES cell-derived motoneurons in an *in vitro* coculture system and after transplanting them into paralyzed animals. We determined that ES cell-derived motoneurons are capable of carrying out fundamental functions of normal motoneurons, including directional growth of long axons, formation of neuromuscular junctions, and induction of muscle contraction. Moreover, we showed that these cells, when transplanted into animals treated with blockers of myelin-mediated axonal inhibition, were capable of growing axons through spinal cord white matter and into the ventral roots of injured animals. To our knowledge, this is the first demonstration of spinal motor axon regeneration in the adult mammalian nervous system. As such, these findings are important steps in developing therapeutic applications of stem cells for spinal cord regeneration.

The adult mammalian spinal cord is a nonneurogenic site, likely because of a nonpermissive environment for the generation of new neurons (3, 7, 23). We committed ES cells to a motor neuron fate before transplantation and found that several thousand ES cell-derived motoneurons survived within the spinal cord of each transplanted rat. Survival of transplanted motoneurons was largely independent of whether we transplanted them into naïve or paralyzed rats, suggesting that the continued differentiation of these cells is independent of environmental cues. This extensive survival of new motoneurons within the adult mammalian spinal cord suggests that the application of *ex vivo* conditioning may allow efficient generation of new neurons in nonneurogenic regions of the neuraxis.

However, to achieve reinnervation of skeletal muscle targets *in vivo*, many additional hurdles needed to be overcome. First, the biology of ES cell-derived axonal extension within the adult mammalian spinal cord must be understood and we found for the first time, to our knowledge, that CNS myelin inhibits growth of ES cell-derived axons. The adult mammalian CNS has a limited capacity for nerve regeneration, due, at least in part, to the presence of three myelin-associated inhibitors of axonal growth: myelin-associated glycoprotein, Nogo-A, and oligodendrocyte-myelin glycoprotein. All three versions of Nogo, oligodendrocyte-myelin glycoprotein, and myelin-associated glycoprotein bind with high affinity to the Nogo-66 receptor, a glycophosphatidylinositol-linked surface protein, and likely transmit a signal through the P75 neurotrophin receptor (24). Signaling via this pathway may decrease intraneuronal cAMP (25) and differentially activate members of the Rho GTPase family. In the active state, the Rho GTPases bind a set of effector molecules, including the serine-threonine kinase Rho kinase (26). Rho kinase negatively regulates growth cone motility by phosphorylating myosin light-chain phosphatase (27) and myosin light chain itself (28, 29).

Because we saw that ES cell-derived axon growth was inhibited by myelin, we investigated pharmacologic strategies to reduce this inhibition. Several such strategies have been recently applied to

stimulate axonal growth of native neurons within the mammalian nervous system (25, 30–33). Inhibition of RhoA activity by C3 transferase or use of a dominant-negative inhibitor of Rho kinase activity abolished the inhibitory activity of myelin-associated glycoprotein and Nogo-A (34). Additionally, Y27632 abolished all of the inhibitory activity of myelin-associated glycoprotein and 60–70% of inhibition mediated by the two active regions of the Nogo-4 (29). Arginase I and polyamines are also downstream effectors of the cAMP axonal outgrowth pathway, although their exact roles remain unclear (33).

We found that ES cell-derived motoneurons are responsive to some of the same cues as native neurons and by treating paralyzed animals with dbcAMP, ES cell-derived motoneurons extend axons through CNS white matter and into the peripheral nervous system. To our knowledge, this is the first demonstration that transplanted neurons can be induced to extend axons into the peripheral nervous system. However, we estimate that only 2.4% of ES cell-derived motoneurons extended axons into the peripheral nervous system and, therefore, additional strategies must be used to enhance the efficiency of this process. Because we have previously shown that 80–85% of ventral root axons are eliminated by NSV infection (6), steric hindrance is unlikely to account for this inefficiency. Rather, it is possible that removal of myelin-mediated repulsion needs to be coupled with attractive cues from the acutely denervated peripheral nervous system. Perhaps the most interesting signaling molecules in the context of axonal regeneration are the neurotrophins, because of their ability to act on the mature adult spinal cord and to act at a distance. Several neurotrophic factors, including nerve growth factor, NT-3, brain-derived neurotrophic factor, and glial-derived neurotrophic factor have been shown to promote and guide axonal regrowth in a variety of contexts (25, 35, 36). Therefore, future work is warranted.

Although we did not see formation of neuromuscular junctions by transplanted ES cell-derived motor axons *in vivo*, *in vitro* studies described in the current work strongly suggest that these cells do have the capacity to do so. Cocultured ES cell-derived motoneurons and skeletal muscle-derived myoblasts exhibited cellular changes, suggesting that these two cell types were responding to cues from each other, resulting in further differentiation of each. Furthermore, we saw aggregation of acetylcholine receptors, where the ES cell-derived axon contacted the muscle fiber membrane and subsequent contraction of the muscle fibers. Formation of neuromuscular junctions is a complex process involving numerous signaling pathways initiated by both the muscle and the neurons. Initial acetylcholine receptor aggregation may occur along skeletal muscle fibers independently of neural signaling (37, 38), but maintenance of this clustering requires neural agrin and other neurally secreted signals (e.g., neuregulin) through activation of positive-feedback loops (39, 40). Agrins and FGF-2 may also be involved in neurite outgrowth (41) in coculture and again, further exploration as to whether these or other signals mediate the axonal guidance of ES cell-derived motoneurons to muscle is warranted.

Therapeutic use of stem cells to regenerate motoneurons in the spinal cord will require that stem cells are efficiently delivered to the injured area, differentiate into motoneurons that survive for extended periods of time, and send axons through the white matter toward muscle targets. We have shown all of these in the current study. Future studies must examine whether ES cell-derived axons can extend toward anatomically and functionally appropriate distal muscle targets and whether they can form junctions upon reaching these muscles. Furthermore, it will be necessary to establish that host motor, sensory, and interneurons can form synapses upon transplanted motoneurons, thus integrating them into appropriate neural circuits.

We thank the Families of Spinal Muscular Atrophy, Andrew's Buddies/Fight Spinal Muscular Atrophy, Robert Packard Center for ALS Research at Johns Hopkins, and the Katie Sandler Fund for Research at Johns Hopkins for their support. We thank Pamela Talalay for a critical review of this manuscript.

1. Flax, J. D., Aurora, S., Yang, C., Simonin, C., Wills, A. M., Billinghurst, L. L., Jendoubi, M., Sidman, R. L., Wolfe, J. H., Kim, S. U., *et al.* (1998) *Nat. Biotechnol.* **16,** 1033–1039.
2. Zhang, S. C., Wernig, M., Duncan, I. D., Brustle, O. & Thomson, J. A. (2001) *Nat. Biotechnol.* **19,** 1129–1133.
3. Shihabuddin, L. S., Horner, P. J., Ray, J. & Gage, F. H. (2000) *J. Neurosci.* **20,** 8727–8735.
4. Fricker, R. A., Carpenter, M. K., Winkler, C., Greco, C., Gates, M. A. & Bjorklund, A. (1999) *J. Neurosci.* **19,** 5990–6005.
5. Brustle, O., Choudhary, K., Karram, K., Huttner, A., Murray, K., Dubois-Dalcq, M. & McKay, R. D. (1998) *Nat. Biotechnol.* **16,** 1040–1044.
6. Kerr, D. A., Llado, J., Shamblott, M. J., Maragakis, N. J., Irani, D. N., Crawford, T. O., Krishnan, C., Dike, S., Gearhart, J. D. & Rothstein, J. D. (2003) *J. Neurosci.* **23,** 5131–5140.
7. Song, H., Stevens, C. F. & Gage, F. H. (2002) *Nature* **417,** 39–44.
8. Bain, G., Ray, W. J., Yao, M. & Gottlieb, D. I. (1996) *Biochem. Biophys. Res. Commun.* **223,** 691–694.
9. McDonald, J. W., Liu, X. Z., Qu, Y., Liu, S., Mickey, S. K., Turetsky, D., Gottlieb, D. I. & Choi, D. W. (1999) *Nat. Med.* **5,** 1410–1412.
10. Liu, S., Qu, Y., Stewart, T. J., Howard, M. J., Chakrabortty, S., Holekamp, T. F. & McDonald, J. W. (2000) *Proc. Natl. Acad. Sci. USA* **97,** 6126–6131.
11. Wu, P., Tarasenko, Y. I., Gu, Y., Huang, L. Y., Coggeshall, R. E. & Yu, Y. (2002) *Nat. Neurosci.* **5,** 1271–1278.
12. Wichterle, H., Lieberam, I., Porter, J. A. & Jessell, T. M. (2002) *Cell* **110,** 385–397.
13. Fournier, A. E., Takizawa, B. T. & Strittmatter, S. M. (2003) *J. Neurosci.* **23,** 1416–1423.
14. McKerracher, L., David, S., Jackson, D. L., Kottis, V., Dunn, R. J. & Braun, P. E. (1994) *Neuron* **13,** 805–811.
15. Campenot, R. B. (1992) in *Cell-Cell Interactions: A Practical Approach*, eds. Stevenson, B. R., Gallin, W. J. & Hall, D. L. (Oxford Univ. Press, New York), pp. 275–298.
16. Ruegg, M. A. & Bixby, J. L. (1998) *Trends Neurosci.* **21,** 22–27.
17. Chang, D., Woo, J. S., Campanelli, J., Scheller, R. H. & Ignatius, M. J. (1997) *Dev. Biol.* **181,** 21–35.
18. Campagna, J. A., Ruegg, M. A. & Bixby, J. L. (1997) *Eur. J. Neurosci.* **9,** 2269–2283.
19. Liu, D. W. & Westerfield, M. (1990) *J. Neurosci.* **10,** 3947–3959.
20. Pumplin, D. W. (1989) *J. Cell Biol.* **109,** 739–753.
21. Kerr, D. A., Larsen, T., Cook, S. H., Fannjiang, Y. R., Choi, E., Griffin, D. E., Hardwick, J. M. & Irani, D. N. (2002) *J. Virol.* **76,** 10393–10400.
22. Vyas, A. A., Patel, H. V., Fromholt, S. E., Heffer-Lauc, M., Vyas, K. A., Dang, J., Schachner, M. & Schnaar, R. L. (2002) *Proc. Natl. Acad. Sci. USA* **99,** 8412–8417.
23. Horner, P. J., Power, A. E., Kempermann, G., Kuhn, H. G., Palmer, T. D., Winkler, J., Thal, L. J. & Gage, F. H. (2000) *J. Neurosci.* **20,** 2218–2228.
24. Filbin, M. T. (2003) *Nat. Rev. Neurosci.* **4,** 703–713.
25. Cai, D., Shen, Y., De Bellard, M., Tang, S. & Filbin, M. T. (1999) *Neuron* **22,** 89–101.
26. Bito, H., Furuyashiki, T., Ishihara, H., Shibasaki, Y., Ohashi, K., Mizuno, K., Maekawa, M., Ishizaki, T. & Narumiya, S. (2000) *Neuron* **26,** 431–441.
27. Kimura, K., Ito, M., Amano, M., Chihara, K., Fukata, Y., Nakafuku, M., Yamamori, B., Feng, J., Nakano, T., Okawa, K., *et al.* (1996) *Science* **273,** 245–248.
28. Amano, M., Ito, M., Kimura, K., Fukata, Y., Chihara, K., Nakano, T., Matsuura, Y. & Kaibuchi, K. (1996) *J. Biol. Chem.* **271,** 20246–20249.
29. Niederost, B., Oertle, T., Fritsche, J., McKinney, R. A. & Bandtlow, C. E. (2002) *J. Neurosci.* **22,** 10368–10376.
30. Neumann, S., Bradke, F., Tessier-Lavigne, M. & Basbaum, A. I. (2002) *Neuron* **34,** 885–893.
31. Qiu, J., Cai, D., Dai, H., McAtee, M., Hoffman, P. N., Bregman, B. S. & Filbin, M. T. (2002) *Neuron* **34,** 895–903.
32. Lehmann, M., Fournier, A., Selles-Navarro, I., Dergham, P., Sebok, A., Leclerc, N., Tigyi, G. & McKerracher, L. (1999) *J. Neurosci.* **19,** 7537–7547.
33. Cai, D., Deng, K., Mellado, W., Lee, J., Ratan, R. R. & Filbin, M. T. (2002) *Neuron* **35,** 711–719.
34. Spencer, T., Domeniconi, M., Cao, Z. & Filbin, M. T. (2003) *Curr. Opin. Neurobiol.* **13,** 133–139.
35. Ramer, M. S., Priestley, J. V. & McMahon, S. B. (2000) *Nature* **403,** 312–316.
36. Lu, P., Jones, L. L., Snyder, E. Y. & Tuszynski, M. H. (2003) *Exp. Neurol.* **181,** 115–129.
37. Hall, Z. W. & Sanes, J. R. (1993) *Cell* **72,** Suppl., 99–121.
38. Sanes, J. R. & Lichtman, J. W. (2001) *Nat. Rev. Neurosci.* **2,** 791–805.
39. Sander, A., Hesser, B. A. & Witzemann, V. (2001) *J. Cell Biol.* **155,** 1287–1296.
40. Moore, C., Leu, M., Muller, U. & Brenner, H. R. (2001) *Proc. Natl. Acad. Sci. USA* **98,** 14655–14660.
41. Jung, K. M., Cotman, S. L., Halfter, W. & Cole, G. J. (2003) *J. Neurobiol.* **55,** 261–277.